Journal of Molecular Structure 1216 (2020) 128316

Contents lists available at ScienceDirect

Journal of Molecular Structure

journal homepage: http://www.elsevier.com/locate/molstruc

Screening and analysis of bioactive food compounds for modulating the CDK2 protein for cell cycle arrest: Multi-cheminformatics approaches for anticancer therapeutics

Shovonlal Bhowmick [a], Nora Abdullah AlFaris [b, **], Jozaa Zaidan ALTamimi [b], Zeid A. ALOthman [c], Tahany Saleh Aldayel [b], Saikh Mohammad Wabaidur [c], Md Ataul Islam [d, e, f, *]

[a] Department of Chemical Technology, University of Calcutta, 92, A.P.C. Road, Kolkata, 700009, India
[b] Nutrition and Food Science, Department of Physical Sport Science, Princess Nourah Bint Abdulrahman University, P. O. Box 84428, Riyadh, 11671, Saudi Arabia
[c] Department of Chemistry, P.O. Box 2455, College of Science, King Saud University, Riyadh, 11451, Saudi Arabia
[d] Division of Pharmacy and Optometry, School of Health Sciences, Faculty of Biology, Medicine and Health, University of Manchester, Oxford Road, Manchester, M13 9PL, United Kingdom
[e] School of Health Sciences, University of Kwazulu-Natal, Westville Campus, Durban, South Africa
[f] Department of Chemical Pathology, Faculty of Health Sciences, University of Pretoria and National Health Laboratory Service Tshwane Academic Division, Pretoria, South Africa

ARTICLE INFO

Article history:
Received 4 February 2020
Received in revised form
30 March 2020
Accepted 21 April 2020
Available online 24 April 2020

Keywords:
CDK2
Cancer
Virtual screening
Molecular docking
Molecular dynamics

ABSTRACT

The cyclin-dependent kinase-2 (CDK2) belongs to the protein kinase family and its overexpression leads to an unusual regulation of cell-cycle which directly linked with hyperproliferation in many cancer cell types. CDK2 activation spontaneously promotes the cell cycle progression and also involved in a large number of cellular processes including cell cycle regulation, DNA replication, DNA damage response and apoptotic pathways, therefore targeting the CDK2 can be reemerged as a therapeutic boulevard to restrain cancer cell proliferation. For the last two decades, emerging evidences suggested that CDK2 inhibition draws out some antitumor/anticancer activity, which has driven the research possibility for developing next-generation newer or cost-effective inhibitors with greater specificity to CDK2. In the current work, compounds from the FooDB - a world's largest food constituents database was retrieved and curated and followed by multi-pharmacoinformatics approaches adopted to find out potential CDK2 inhibitors. The curated dataset was considered for screening through "Virtual Screening Workflow" (VSW) employed in Schrödinger suite. The numbers of cost-effective food constituents were reduced by removing low potential molecules in terms of interaction affinity and further explored for pharmacokinetics analysis. Based on strong binding interaction profiles with the lowest binding interactions affinity and energy values, four food compounds were proposed as CDK2 inhibitors. A number of key analyzing parameters from molecular dynamics (MD) simulations studies were successfully substantiated that all four proposed food compounds can act as CDK2 inhibitors based on their proficient structural and molecular interactions integrity with CDK2 protein following in the active site cavity. Furthermore, the binding free energy was calculated using the MM-PBSA (Molecular Mechanics Poisson-Boltzmann Surface Area) approach from the entire trajectory frames derived in MD simulation revealed strong interaction affinity. The binding free energy was found to be in the range of −991.831 to −210.452 kJ/mol. High binding free energy was undoubtedly explained that all molecules possess strong affection towards CDK2. Hence, proposed molecules may be crucial to stop the hyperproliferation in cancer cells subjected to experimental validation.

* Corresponding author. Division of Pharmacy and Optometry, School of Health Sciences, Faculty of Biology, Medicine and Health, University of Manchester, Oxford Road, Manchester, M13 9PL, United Kingdom.
** Corresponding author.
E-mail addresses: naalfaris@pnu.edu.sa (N.A. AlFaris), ataul.islam80@gmail.com (M.A. Islam).

https://doi.org/10.1016/j.molstruc.2020.128316
0022-2860/

1. Introduction

Over the past decades, based on several physiopathological and clinical studies it has been described that bioactive food compounds shown either a detrimental or beneficial role in many diseases including cancer, type-2 diabetes, obesity, cardiovascular, and neurological disorders [1–6]. Pieces of scientific evidence and epidemiological information support that intake of bioactive natural food products included fruits and vegetables are associated with enhancing potential health benefits [7], including decreased the risk of various chronic diseases [8,9]. For example, some known bioactive compounds which present in food products such as quercetin, gallic acid, ascorbic acid, polyphenols, caffeine, catechins, anthocyanins, oleuropein, capsaicin, resveratrol, epigallocatechin, curcumin, sulforaphane, ellagic acid, b-glucans, and other food containing biomolecules may directly contribute to prevention or improving immunity, treatment, or management of many diseases via modulating different molecular signaling pathways [1,8,10]. However, understanding the possible molecular effects of several bioactive food compounds in the progression of such disease-modifying implications has remained enigmatic [11]. Although, several studies have suggested that a wide array of molecular targets are majorly associated with changes that might constitute the mechanistic possessions for exerting such detrimental or beneficial effects in human health by bioactive food compounds. Even, those associations are not always straightforward due to a large number of metabolites derived from the bioactive food compounds play piles of role in mechanistic changes of metabolic pathways [11,12]. Precisely, a considerable number of clinical trials in the various human cell and tissue samples demonstrated that bioactive food compounds have a strong involvement in selective gene expression and thereby modulating epigenetic modifications [13–15]. Alterations in epigenetic patterns are highly associated with tumorigenesis because epigenetic changes might affect the gene expression at a different level and increase disease susceptibility. An earlier study has suggested that the effects of specific food compounds or dietary nutrients on epigenetics disclose a strong association with increased risk of cancer which can modulate DNA methylation [16]. Large-scale loss of such epigenetic modifications or aberrant DNA methylation is the hallmark of cancer [17,18]. Moreover, bioactive food components are involved in various nutrigenomic or nutritional transcriptomic effect which influences the phosphorylation and post-translational events or other proteomic modifications [19]. Therefore, optimizing the intake of the specific type of bioactive food components seems to be a more prudent, noninvasive, and cost-effective approach for bringing down cancer burden from our society.

Nowadays anti-cancer therapeutic strategies are directly targeting damage DNA or signaling molecules associated with cell division mechanisms due to fact that cancer cells mostly consist of faulty cell cycle checkpoints or they lose the cell cycle rhythm [20]. It is quite obvious that due to integral cellular progression there is a strong connection between the cell cycle and cancer [21,22]. In general, there are four sequential phases which involve in cell division cycles, and each phase tightly maintained by motors of the cell cycle machinery known as cyclin-dependent kinases (CDKs) – belong to the serine/threonine protein kinase family [23]. CDKs, are particular types of enzyme family which use signals to switch on cell cycle mechanisms. Precisely, CDKs are acted upon binding with cyclin protein and involved in various aspects of cell biology including cell-cycle regulation or control, transcription, phosphorylation of RNA polymerase II and metabolism, and certain types of cell differentiation [24]. Among various subfamilies of CDKs, cyclin-dependent kinase 2 (CDK2) plays an important role in the progression of cells to enter into the S- and M-phases during the cell division cycle [24]. Earlier a number of evidences proposed that CDK2 is critically linked with tumor development in multiple cancer types [25–32], and therefore continues to seek special attention to exploit in anticancer drug development [33–35]. It can be postulated that by directly targeting the CDK2 for inhibition or by the means of abrogation of cell cycle checkpoints, thereby an unrestricted cell growth can be inhibited. Therefore, now rationally designing the CDK2 specific inhibitors have gained special attention for the discovery of new anticancer/antitumor agents. Although, few small-molecular chemical entities as CDK2 inhibitors (such as AT7519, AG-024322, CYC065, TG02, Dinaciclib, Roniciclib, Milciclib, as per www.clinicaltrails.gov) have entered into the clinical trials, however, selective CDK2 inhibitor yet to be discovered. As of now, primary analysis on NutriGenomeDB ('Gene expression browser module' search) suggests that there are around 73 different nutrients and bioactive food compounds that have been studied for investigating the modulatory effect of CDK2 gene expression and used for several disease treatment profiles [36,37]. Along with gene expression data, to some extent, the structural knowledge of CDK2 protein is also permitting opportunity for selectively designing the CDK2-inhibitors [38,39]. Like other protein kinases, CDK2 also holds classic bilobal architecture. Amino acid residues 1-81 and 82-297 represent the N-terminal lobe and C-terminal domain, respectively [40]. The N-terminal region mainly consists of β-sheets with one α-helix, whereas the C-terminal domain majorly contains α-helices with the activation segment. A flexible hinge region extend from residues 81(Glu) to residue 84(His), that connect the N-terminal and C-terminal domain together, and which lines a deep cleft, the ATP binding site. Moreover, organized cyclin E-CDK2 complex push towards G_1 progression through the restriction point, which ultimately propel cell cycle completion. Another protein complex CDK2-cyclin A also important to incite cells through the S-phase during cell cycle/division [22]. So, likewise many ways CDK2 or CDKs are responsible for various important biological events during cell cycle in an orderly fashion.

Application of computational resources and power in the drug discovery research has already been reached a new height to discover promising chemical entities for a specific target. Considering the chemical functionalities in terms of pharmacophoric or reactive groups present in the food components having effective anti-cancer activity the current work was studied the multi-step molecular docking based virtual screening of one of the most comprehensive food constituents database *viz.* FooDB against the CDK2. Followed by molecular docking, *in silico* ADME (absorption, distribution, metabolism, excretion) prediction analyses, molecular dynamics (MD) simulations and MM-PBSA (Molecular Mechanics - Poisson–Boltzmann Surface Area) based ligand binding free energy calculations were carried out. Finally, four compounds were identified from FooDB through extensive virtual screening procedures which can act as potential CDK2 modulating agents. So, the credential of the work was substantiated by finding of four potential molecules for successful inhibition of CDK2 protein.

2. Materials and methods

Virtual screening of large chemical databases based on the macromolecular structure has evolved as a crucial drug discovery

weapon supplementing traditional high throughput screening (HTS) methodologies. One of the vital advantages of virtual screening is to reduce the large chemical dataset to the promising set of molecules with extremely less time, low-cost investment and most importantly without animal sacrifice. In the current study, multi-cheminformatics approaches included virtual screening, molecular docking and molecular dynamics simulation were adopted to find out promising CDK2 chemical agents from the food component. For this purpose, a set of 90937 chemical entities from the FooDB (www.foodb.ca) was collected and curated for screening against the CDK2. FooDB is the most widely accessed, prevalent and inclusive food constituents database. This database consisting of a wide range of information on macronutrients and micronutrients, including many of the constituents that give foods their flavor, color, taste, texture and aroma. A large number of compositional, biochemical and physiological information are collected from the literature of each of the components and provided as an information column. Different characteristics including the nomenclature, description, information on its structure, chemical class, physicochemical data, food source(s), color, aroma, taste, physiological effect, presumptive health effects and concentrations in various foods are provided comprehensively. The FooDB is easy to access and can be searched through different keywords including food source, name, descriptors, function or concentrations. Hence, chemical components from FooDB targeting CDK2 can be an excellent approach to modulate the cell cycle arrest. The curated dataset from the FooDB was used for the 'Virtual Screening Workflow' (VSW) [41] in Maestro followed by pharmacokinetics analyses. Finally, selected molecules were further used for MD simulation analyses to explore the behavior of the molecules in dynamic states.

2.1. Preparation of molecular database and CDK2 protein structure

The entire dataset of chemical compounds from the FooDB database was downloaded in SMILES format. Initially, the dataset was curated to remove the redundancies, bad valency and having extremely low molecular weight. After successful curation, a total of 20332 molecules were considered for VSW [41]. The SMILES format of the molecules were converted into structural data format (sdf) using the open-source file format conversion tool, the Open Babel [42]. To validate and compare the outcomes, an established CDK2 inhibitor, Dinaciclib [43] was used as a control molecule throughout the study. The entire dataset and Dinaciclib were prepared using the LigPrep module [44] of Maestro.

The crystal structure of CDK2 protein was collected from the RCSB Protein Data Bank (PDB) with PDB ID: 4KD1 [45]. A number of criteria were adopted to select the CDK2 receptor including resolution and R-value of the molecule, and date of deposition in the RCSB-PDB. The resolution and R-value of the selected protein were found to be 1.7 Å and 0.232, respectively. As per RCSB-PDB record, the selected protein was deposited in April 2013. The Protein Preparation Wizard of Maestro [44] was used to prepare the protein. During the preparation step, the appropriate bond order was assigned for the CDK2 crystal structure and hydrogen atoms added. The missing side chains and loops were repaired. Further, the protein structure was optimized and minimized. Thereafter, protein active site selection was made based on the information of surrounding residues where Dinaciclib binds tightly with CDK2 protein through an intricate network. Precisely, few important amino acid residues such as Ile10, Val18, Ala31, Lys33, Val64, Phe80, Glu81, Phe82, Leu83, Lys89, Gln131, Asn132, Leu134, and Asp145, etc. were selected as active site residues which likely to be responsible for the binding mechanism [45–49]. Overall, these selected active site residues in CDK2 are covering several important regions includes ATP binding site, hinge region, p-loop region, strictly conserved residue, gatekeeper residue, and also DFG motif of the kinase. Hence, specified region and amino acid residues around the co-crystal bound Dinaciclib was considered as a potential active site in the current study. Finally, the grid box was generated using the Receptor Grid Generation module in Maestro [50] confining the selected residues and area around the co-crystal ligand, Dinaciclib.

2.2. Virtual screening using 'virtual screening workflow' (VSW) and docking validation

The VSW utility available in the Schrödinger suite [50] was used to extensively filter out the chemical compounds obtained from the FooDB. The comprehensive VSW utility tool is the part of the Grid-based Ligand Docking with Energetics (Glide) module [51] available in the Schrödinger suite [50] and rigorously used for virtual screening of large molecular dataset. The VSW includes ligand preparation, initially filtering of compounds based on pharmacologically relevant parameters, and followed by up to three different docking protocols i.e. progressing from Glide-high-throughput virtual screening (HTVS), standard precision (SP), and extra precision (XP) docking for competently and consistently finding out the set of potential chemical entities with high precision [52]. The entire execution of VSW protocol embedded in the Schrödinger suite was performed in the CHPC server, Cape Town, South Africa (https://www.chpc.ac.za/index.php/resources/lengau-cluster). In order to run the workflow, some specific parameters and options were selected and considered as input in VSW panel. Curated molecules from the FooDB were taken as input in the VSW for the source of ligand files under 'Input' tab and no specific filtering criteria considered at this stage. All ligands were allowed to prepare in the 'Preparation' tab option to generate the 3D coordinates of each ligand. The grid file generated by confining the bound ligand was browsed through the 'Receptor' tab. In the case of Glide-HTVS docking, a total of 10% best docked ligands was considered for proceeding with the next step. Total of 10% best docked ligands in SP docking mode were carried forward for the XP-docking procedure. Finally, 40% of best docked molecules in the XP-docking method were kept and 'write XP descriptor information' selected as output file creation. Moreover, in the entire process of VSW 'all good scoring states' were held for ligand-protein complexes. The remaining parameters in the workflow were kept as default. After successful screening in VSW, the leftover molecules were adopted to calculate the binding free energy using Prime MM-GBSA method. The Glide-XP score and binding energy calculated through MM-GBSA approach were explored and the top-ranked food chemical components selected for further analyses.

2.3. In-silico ADME and drug-likeness prediction

The pharmacokinetics analyses is an important approach to screen out drug-like molecules against a particular target. On successful screening of the FooDB molecules through VSW, the remaining molecules were subjected to the pharmacokinetics analyses in SwissADME web server [53], available at http://www.swissadme.ch/. The SwissADME is widely used and favorite pharmacokinetics analysis tool to the scientific community due to steadfast predictive power and impulsive straightforward interpretation. A number of physicochemical and drug-likeness properties including properties under Ro5 [54] were recorded to explore acceptable pharmacokinetics profiles. Moreover, several other important pharmacokinetics features included n-octanol and water (log $P_{o/w}$) partition coefficient or lipophilicity, molar solubility in water, blood-brain barrier (BBB) permeability, skin permeation, human gastrointestinal absorption (HIA) capability were critically explored to finalize best CDK2 inhibitors.

2.4. Molecular dynamics simulation and binding free energy through MM-PBSA approach

The MD simulation is the crucial and essential approach to explore the dynamic nature of any protein-ligand complex. Finally selected CDK2 inhibitors bound with the same were used to all-atom 100ns MD simulation study with a time step of 2 fs at the constant pressure of 1 atm and constant temperature of 300 K. The MD simulation study was performed in the Gromacs 2018.2 software tool (http://www.gromacs.org/) available at the Lengau CHPC server. In order to generate the ligand topology the online freely available, SwissParam tool [53] was used. All-atom CHARMM36 force field was considered to generate the protein topology. Prior to the simulation, the protein-ligand complex was confined within a cubic box with a diameter of 1 Å from the center of the system. To solvate the system the TIP3P water model was used. The system was neutralized by the external addition of a required number of Na^+ and Cl^- ions. To equilibrate the system, the steepest descent algorithm of 10,000 steps was applied followed by the minimization of each system. To consider van der Waals and electrostatic the cut off were used to 0.9 and 1.4 nm correspondingly for the long-range interaction parameter. The snapshots after each of the 1ps intervals were recorded to explore the trajectory information. After successful completion of the MD simulation, the behavior of the system and complex were analyzed through a number of parameters included root-mean-square deviation (RMSD), root-mean-square fluctuation (RMSF) and radius of gyration (Rg). The whole MD simulation trajectories were used to calculate the binding free energy through the MM-PBSA (Molecular Mechanics Poisson-Boltzmann Surface Area) approach using g_mmpbsa utility tool [55]. Detailed method and procedure to calculate the binding free energy through MM-PBSA can be found in one of the previous publications by our research group [56].

3. Results and discussion

3.1. Virtual screening through 'virtual screening workflow'

Screening of large molecular databases through structure-based paradigm is becoming a popular and pivotal approach in modern drug discovery research. The availability of such a large number of the crystal structure of macromolecules is a pioneering step to start the structure-based virtual screening. In the current study, a curated dataset of 20332 molecules belong to the food constituents were collected from the FooDB.

The CDK2 protein structure was obtained from the RCSB-PDB (PDB ID: 4KD1) and considered for molecular modeling study [45]. The VSW implemented in the Maestro [41] was used to reduce the chemical space and selection of potential CDK2 inhibitors. In VSW, a multistep-docking approach was used such as HTVS, SP and XP followed by binding energy calculation through MM-GBSA approach. The flow diagram of the work is given in Fig. 1. It is essential and crucial to validate the docking protocol before employing any molecular docking-based virtual screening study. The self-docking is an approach which widely and commonly used for the molecular docking protocol validation. Herein, the bound co-crystal small molecule was re-drawn and docked at the same active site where it originally bound in the protein. The protocol which can produce a similar orientation to the co-crystal ligand can be considered as suitable for the molecular docking of any unknown set of ligands. It is also reported that the RMSD value of <2 Å obtained from the superimposed co-crystal and docked ligand successfully validate the molecular docking protocol [57]. In the current study, co-crystal bound ligand Dinaciclib was re-docked using VSW where three levels of molecular docking such as

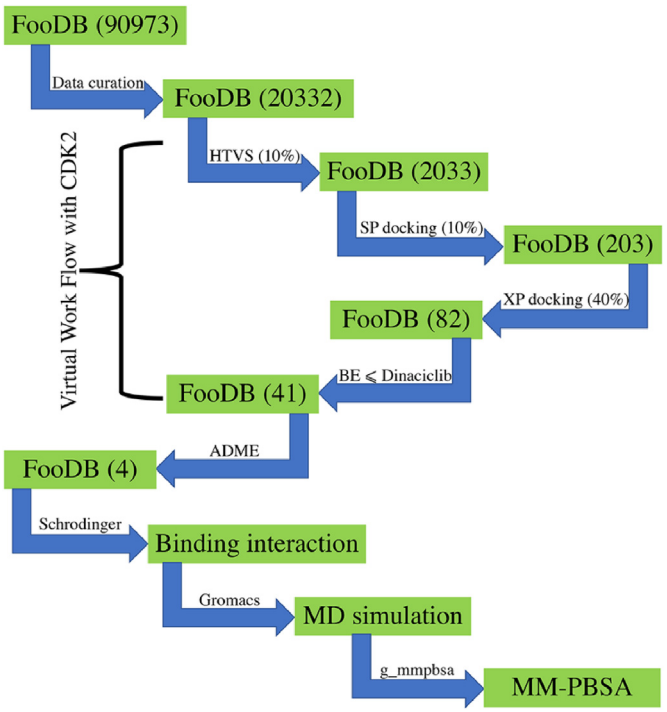

Fig. 1. Schematic workflow of the virtual screening proceedure of FooDB molecules against CDK2.

Glide-HTVS, Glide-SP and Glise-XP was embedded. In each step the 100% docked compound kept to get all possible docked poses for Dinaciclib inside the CDK2 cavity. The best-docked pose of Dinaciclib and co-crystal Dinaciclib were superimposed and RMSD found to be 0.892 Å. The obtained RMSD value was clearly indicated that considered molecular docking protocol successfully validated. Hence, it was expected that docking of any molecule inside the CDK2 using the same protocol can provide true positive docked orientation for the newly docked molecule. Therefore, the same protocol was applied for the docking of the entire food compound dataset inside the CDK2. The superimposed co-crystal structure of Dinaciclib and best re-docked pose of Dinaciclib is presented in Fig. S1 (Supplementary file).

Two parameters such as binding interactions and dock score were used to assess the molecules passing through VSW. A total number of 20332 curated molecules were allowed for HTVS protocol and the best 10% food constituents selected for the next step consideration in docking study. Remaining molecules after HTVS (2033) were used for SP docking and again best 10% molecules retained for the XP-docking. A total of 203 molecules were used for the XP-docking and best 40% retained for further analyses. Finally, the binding energy of all molecules obtained after XP-docking (82 compounds) was calculated through the MM-GBSA module. The binding energy of standard compound Dinaciclib was calculated and found to be −45.543 kcal/mol. Therefore, molecules having binding energy values less than −45.543 kcal/mol were considered for subsequent analyses. It was found that a total of 41 molecules having binding energy less than −45.543 kcal/mol. Moreover, all 41 selected molecules were further assessed through *in-silico* pharmacokinetics analyses and results presented in Table S1 (Supplementary file). Based on acceptable absorption, distribution and metabolism and medicinal chemistry profiles finally four molecules were selected as promising CDK2 inhibitors and subjected for MD simulations analyses. The two-dimensional (2D) representation of proposed CDK2 inhibitors (A1-A4) is given in Fig. 2.

3.2. Molecular docking predicted interaction analysis of identified food compounds

Four compounds (Compounds A1-A4 in Fig. 2) were selected based on the highest negative docking and MM-GBSA scores against the docked complexes obtained in VSW analysis. The selection of each compound pose was retrieved based on all negative docking score (better than the standard compound Dinaciclib), and their respective docked conformations along with best dock conformation of Dinaciclib-CDK2 complex. The binding interactions profile of A1, A2, A3, A4 and Dinaciclib are given in Fig. 3. It was revealed that A1 formed number of molecular interactions profile with CDK2 at its active site. Particularly, residue Leu83 was formed two hydrogen bond (H-bond) interactions at the bond distances of 1.96 and 1.72, respectively, and Gln131 also found to be involved in H-bond interaction at the distance of 2.22 Å. It was found that one hydroxyl group present in A1 formed two H-bond interactions with residue Leu83. A number of other active site residues (Ile10, Val18, Ala31, Gln131 and Leu134) participated in hydrophobic interactions with A1. Binding interaction analysis also revealed that A1 was also established water and salt bridge interactions with residue Asn132 and conserved basic residue Lys33, respectively. Another basic amino acid residue Lys89 of CDK2 was found to participate in both types of molecular interactions (water and salt bridge) with A1. The visual binding orientation of A2 was confirmed that amino acid residues Glu12, Lys33, Glu81, Leu83, Asp86 and Gln131 participated in H-bond interactions. Mostly the hydroxyl functional groups present in bioactive food compound A2 participated to form H-bond interactions. The bond distance of the H-bond interactions for residues Glu12, Lys33, Glu81, Leu83, Asp86 and Gln131 was measured as 2.21, 1.56, 1.83, 1.69, 1.91 and 2.29 Å, respectively. The H-bond interaction associations with the above residues undoubtedly were influenced in protein stability upon binding of A2 with CDK2 protein and hence to form a stable complex. Moreover, it was observed that above mentioned binding interactions specifically created at the hinge-region (residues 81–83) of the ATP binding site and also with conserved residue (Lys33) of CDK2. Such a profound interaction orientation for A2 strongly supports its high selectivity for being the CDK2 inhibitor. Alike A1, hydrophobic interactions were also found for A2 with the active site residues (Ala31 and Gln131) of CDK2 protein. Usually, the narrow hydrophobic cavity formed by residues Ala31 and Leu134 of CDK2 commonly seems appropriate for binding of any hetero-aromatic rings. In this study, aromatic rings present in A2 specifically formed hydrophobic contacts with Ala31 and Gln131 amino acid residues. Exploration of binding interactions profile of A3 displayed three types of molecular interactions profile *viz.* H-bond, hydrophobic and water bridge interactions with CDK2 protein.

Compound A3 formed a number of H-bond interactions with residues Ile10, Glu12, Leu83, Lys89, and Gln131, whereas hydrophobic interactions was observed with residues Val18, Ala31, and Leu134. The observed H-bond distances for the residues Ile10, Glu12, Leu83, Lys89, and Gln131 were noted as 2.63, 1.76, 2.12, 2.06 and 1.86 Å, respectively. In addition, water bridge interactions were also formed with A3 through Thr14, Gln131 and Asn132 amino acid residues of CDK2 protein. Compound A4 formed H-bond interaction with five amino acid residues (Glu12, Lys33, Leu83, Asp86, and Lys89). The H-bond distances for all residues *viz.* Glu12, Lys33, Leu83, Asp86, and Lys89 formed interactions with A4 measured as 2.39, 2.21, 1.96, 1.79, and 2.04 Å, respectively. Apart from the H-bond interactions, four residues (Ile10, Ala31, Gln131, and Leu134) were participated to form hydrophobic contacts with A4. As already explained that side chains of these residues (Ala31 Gln131 and Leu134) were mostly involved in shaping deep hydrophobic cavity for CDK2, and therefore several aromatic rings present in A4 also favors the formation of hydrophobic contacts in that specific binding site. Only two types of molecular interaction profiles (H-bond and hydrophobic interactions) were observed for the standard compound Dinaciclib in docking analysis. It was noticed that only two residues (Leu83 and Gln131) were formed three H-bond interactions with the measured bond distances of 1.98, 2.02 Å (for Leu83), and 2.21 Å for Gln131, whereas amino acid residues Val18, Ala31, Phe80, Gln131, Leu134, and Ala144 involved in hydrophobic interactions. The obtained docking interactions profile for the standard compound Dinaciclib was found to be highly likely similar to many as other studies reported earlier [45,58,59] and such

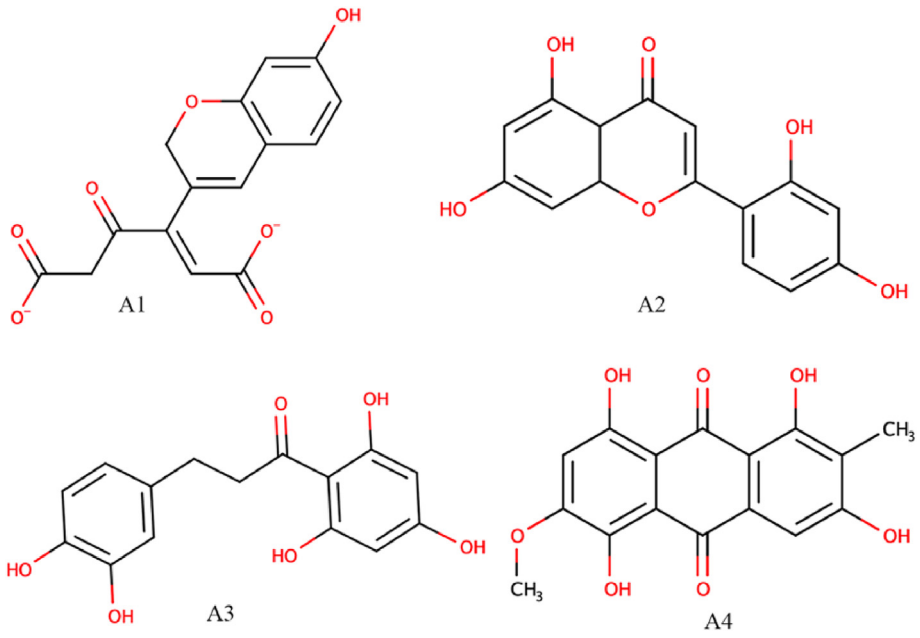

Fig. 2. Two-dimensional representation of finally selected bioactive food compounds as CDK2 inhibitors.

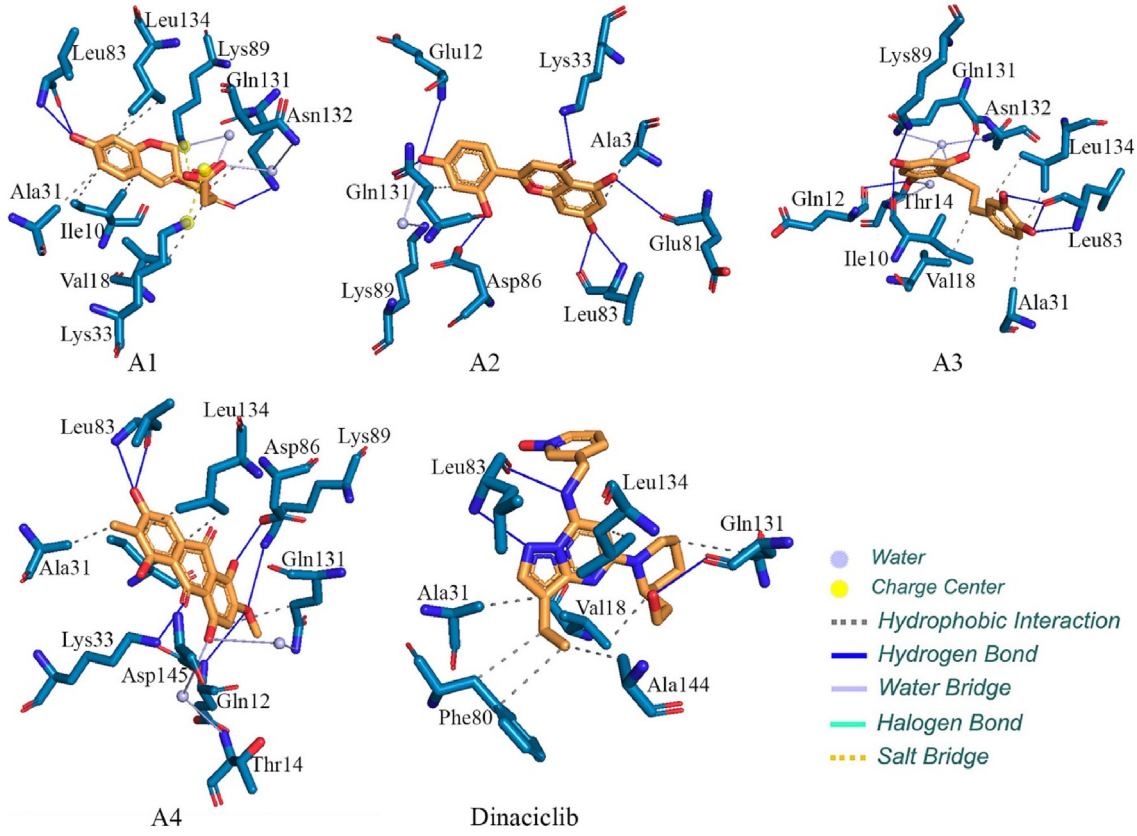

Fig. 3. Molecular binding interactions of A1, A2, A3, A4 and Dinaciclib with CDK2 obtained from XP-docking study.

instance also supports the successful docking protocol validation indirectly. The XP-Glide dock score was found to be −10.62, −10.16, −10.21, −9.43, and −9.17 kcal/mol for A1, A2, A3, A4 and Dinaciclib, respectively. Overall, the study findings revealed much greater and better molecular interactions profile for all identified bioactive food compounds (A1-A4) in terms of docking and MM-GBSA scores in comparison to standard compounds.

In particular, few interesting observations of the docking study were ascertained as the involvement of amino acid residue Leu83 as a common residue which formed H-bond interactions with all the identified food compounds. As amino acid residues 81-83 constitute a flexible hinge region and also connect the C- and N-terminal domain of CDK2 and specifically Leu83 also responsible for ATP binding site, therefore, any type of molecular binding interactions with residue Leu83 might be crucial for exhibiting binding stability as well as binding free energies of the identified inhibitors. Notably, these findings were undoubtedly explained the high potency and selectivity of the identified compounds towards CDK2. Earlier several studies also reported the pivotal role of the same amino acid (Leu83) associations in explicating the CDK2 inhibitory activity [60–63]. Apart from this observation, another important amino acid residue Gln131 also took part in stabilizing the conformational integrity by forming the H-bond interaction with all food compounds except A4. Most of the H-bond interactions observed for this residue as the attachment of carbonyl group of Gln131 with oxygen atom of the identified food compounds. Similar study findings also revealed by other research groups [58,64,65] clearly explained that proposed molecules constitute the potential structural features for being crucial CDK2 inhibitors. The presence of water molecules in the active site cavity of CDK2 play a crucial role to interact with the ligands [66]. A number of ways water molecules can interact with protein and ligands included by the formation of water bridge with either or both protein and ligand, interaction with protein and ligands through hydrogen bonding separately, and, presence of free water molecules [67]. It is illustrated that among all above the water bridge is the most prevalent type of interaction for the CDK2 and ligand complex [68]. On detailed observation, it can be seen that proposed all four ligands and few catalytic amino residues were formed a number of water bridges to stabilize the molecules inside the receptor cavity of CDK2. From Fig. 3, it can be seen that individually A1, A3 and A4 were formed two water bridges, while A2 established one. Amino residue, Asn132 was established water bridge when CDK2 bound with A1 and A3. The Lys89 clashed with water in case of CDK2 complex with A1 and A4. The water bridge was also seen to be formed with Thr14 and Gln131 in CDK2 complex with A3 and A4. Moreover, Asp86 was found to be crucial to form water bridge in case of the complex CDK2 and A2. The above observation absolutely explained that water bridges with protein and all proposed molecules were played an important role to stabilize the protein-ligand complexes. To deduce better insight about the binding modes, surface view orientation and as well as three dimensional ligand-protein contact maps in cartoon representation were generated and checked carefully for all compounds and depicted in Fig. 4.

Interestingly, it was observed that all proposed molecules and as well as standard compound Dinaciclib perfectly occupied inside the receptor cavity space of the CDK2 protein. Although, the standard compound Dinaciclib fitted inside the CDK2 receptor cavity, however, its binding orientation looks bit different from the identified compounds (A1-A4). It appears that some parts of compounds Dinaciclib more prone to bind through the solvent-exposed cavity area. Notably, such observation was corroborated with earlier

reported literature [45] where the structural basis for the high potency and selectivity of Dinaciclib were extensively studied against CDK2.

3.3. Molecular similarity analyses

The structural similarities among all the identified bioactive food compounds as the CDK2 inhibitors were carried out. As molecular structural similarity principle [69] implies that more structurally similar molecules inclined to have alike physicochemical as well as biological properties, although, there are some exceptions as well. The concept of molecular structural similarity encompasses several components such as atomic positions, bonding patterns, shape, conformation, and spatial disposition of molecular properties, etc. In order to get the similarity correlation among the identified compounds, herein ChemMine Tools [70] was used which measures structural similarities based on the multidimensional scaling (MDS) clustering method. In particular, MDS clustering method calculated structural similarities by all-against-all comparisons for all given input compounds using atom pair similarity measures and later on transforming the yielded similarity scores into distance values. Employing such a rigorous algorithm for structural similarity evaluation, it was found that three compounds (viz. compounds A1, A2 and A3) seems structurally more similar than A4. The graphically represented scatter plot in two-dimensional space (given in Fig. S2 in Supplementary file) clearly demonstrated their structural relatedness obtained based on matrix of item-item distances. Moreover, structural similarity or dissimilarity based on physicochemical/structural properties were explored and suggested few differences among all compounds. In terms of atomic associations, it was found that A1, A2 and A3 consist of 15 carbon atoms, in contrast, A4 consists of 16. In a similar fashion, the number of oxygen atoms was found to be 7, 6, 6, and 7 in A1, A2, A3 and A4 respectively. Interestingly, only A1 holds two negatively charged ions (O^-) which might be exceptional but could be crucial for influencing the movement of ions and molecules across the plasma membrane and hence maintain chemical equilibrium in the cell. Moreover, from the structural aspect, another important component such as the presence of numbers of aromatic rings was counted as 1, 3, 2 and 3 for A1, A2, A3 and A4, respectively.

3.4. Pharmacokinetics analysis

In order to explore the potentiality of the proposed CDK2 inhibitors, the pharmacokinetics and physicochemical properties were analyzed using the SwissADME web server [53]. All recorded characteristics are given in Table 1. The molecular weight of A1, A2, A3 and A4 was found to be 304.25, 286.24, 274.27 and 316.26 g/mol,

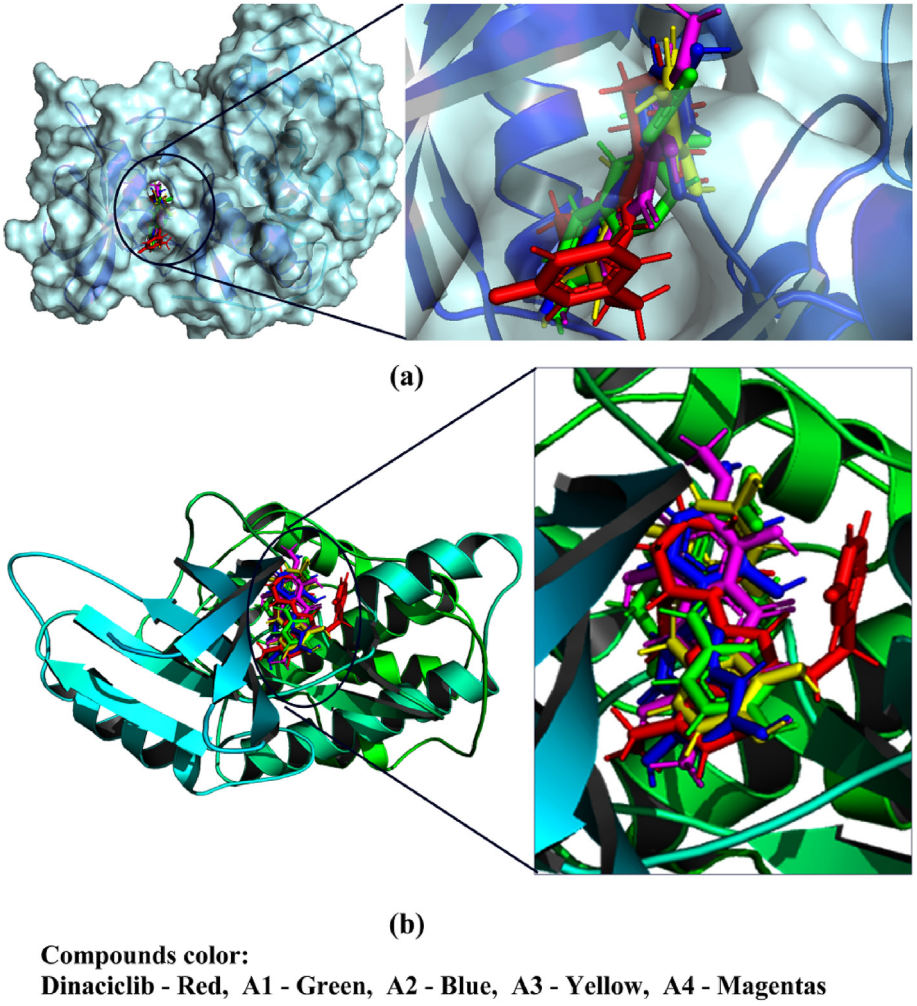

Fig. 4. (a): Binding interface of compounds A1, A2, A3, A4 and Dinaciclib with CDK2 in surface view orientation; (b): XP-Glide based binding mode of compounds A1, A2, A3, A4 and Dinaciclib (as stick) with CDK2 (as cartoon representation).

respectively which indicated that size of the molecule as per recommended by Ro5. The topological polar surface area less than 140 Å^2 explains the oral activeness of any molecule. The proposed molecules were found to have a polar surface area between 97.99 and 124.29 Å^2 that undoubtedly enlightens that all molecules orally active in nature. The solubility of the molecules was analyzed and found that all molecules soluble in nature. The human intestinal absorption (GI) and blood-brain barrier (BBB) parameters clearly explained that each and every molecule were possessed high absorbable characteristics. Not a single molecule was found to violate the Ro5, Ghosh's and Veber's rule. The number of rotatable bonds explains the flexibility of the molecule.

It was found that A1, A2, A3 and A4 contain numbers of rotatable bonds of 5, 1, 4 and 1, respectively, which clearly explained that flexibility of A1 and A3 more in comparison to A2 and A4. In addition to the above HIA and BBB were further analyzed and portrayed BOILED-Egg model in Fig. 5. The BOILED-Egg model was represented by albumin (white) and yolk (yellow) regions. Molecules present in the albumin region considered to be more HIA penetration, while, in yolk region more BBB penetration. It is also illustrated that yellow and white regions are not mutually exclusive. From the above explanations and Fig. 5 it can be seen that all molecules were showed strong absorption in the HIA. Another important parameter, substrates (PGP+) and non-substrates (PGP-) of the permeability glycoprotein (PGP) can also be explained in Fig. 6. In Fig. 6, the PGP+ and PGP- characteristics are represented by blue and red circles, respectively. It is illustrated that on drives back the molecules into the intestinal lumen in the liver the PGP decreases the efficiency of PGP+. All compounds, A1, A2, A3 and A4 were found to be in the category of PGP- hence they belong to the non-substrate. The parameters of pharmacokinetics and drug-likeness analyses clearly explained that A1, A2, A3 and A4 consist of characteristics to be potential CDK2 inhibitors.

Table 1
Different physiochemical and ADME parameters of proposed identified food compounds as CDK2 inhibitors.

Parameters	A1	A2	A3	A4
Formula	$C_{15}H_{12}O_7$	$C_{15}H_{10}O_6$	$C_{15}H_{14}O_5$	$C_{16}H_{12}O_7$
[a]MW (g/mol)	304.25	286.24	274.27	316.26
[b]NHA	22	21	20	23
[c]NAHA	6	16	12	12
[d]NRB	5	1	4	1
[e]MR	75.05	76.01	74.02	79.30
[f]TPSA (Å^2)	121.13	111.13	97.99	124.29
[g]LogS	−1.96	−3.79	−3.38	−3.94
[h]SC	Soluble	Soluble	Soluble	Soluble
[i]GI	High	High	High	High
[j]BBB	No	No	No	No
[k]vROF	0	0	0	0
[l]vGhose	0	0	0	0
[m]vVeber	0	0	0	0
[n]BS	0.56	0.55	0.55	0.55
[o]SA	3.42	3.06	2.01	2.79
iLOGp	0.73	1.76	1.54	2.05

[a] Molecular weight.
[b] No.of heavy atoms.
[c] No.of aromatic heavy atoms.
[d] No. of rotatable bonds.
[e] Molar refractivity.
[f] Topological polar surface area.
[g] Solubility.
[h] Solubility class.
[i] Gastrointestinal absorption.
[j] Blood Brain Barrier Penetration.
[k] Violation of Lipinski's rule of five.
[l] Violation of Ghose rule.
[m] Violation of Veber rule.
[n] Bioavailability Score.
[o] Synthetic accessibility.

3.5. Molecular dynamics simulation

A 100 ns time span of all-atoms MD simulation was carried out for each of the proposed inhibitors and Dinaciclib complex with CDK2. The MD simulation is an excellent approach to explore the dynamic behavior of the molecules computationally. A number of parameters including RMSD, RMSF and Rg were analyzed from the MD simulation trajectories. Particularly, the analysis of MD trajectories through RMSD parameter provides the overall information on the stability of the protein backbone when bound with the specific ligand/compound during the dynamic condition. In other words, monitoring the RMSD of the protein can provide brief insights into its structural conformation throughout the MD simulation. RMSD analysis also can infer the overall state of the simulation and indicate whether simulation has equilibrated or not. It is implicated that as lower as the RMSD value throughout the MD simulated trajectory suggests high stability of the protein-ligand complex, whereas higher RMSD value indicates comparatively low stability of the protein-ligand complex. Changes in RMSD within the lower range are perfectly acceptable for protein biomolecules. However, changes in larger range might indicate that the protein is probably undergoing large or some sort of conformational change during the simulation. The average, maximum and minimum RMSD, RMSF and Rg values are given in Table 2. The average RMSD value of CDK2 protein backbone atoms complexed with A1, A2, A3, A4 and Dinaciclib was found to be 0.436, 0195, 0.348, 0.175 and 0.187 nm, respectively. Interestingly, no complex was found to have an average RMSD value of more than 0.436 nm. The RMSD value of each and every frame developed during the MD simulation was plotted against the time of simulation and given in Fig. 6. It can be seen from Fig. 6 that the backbone of CDK2 deviated more with respect to the initial structure when bound to A1 and A3. The CDK2 backbone bound with A2, A4 and Dinaciclib remained consistent throughout the MD simulation. The presence of a greater number of rotatable bonds in A1 and A3 might be the possible reason behind such high deviation with respect to the initial conformation. The magnitude of the deviations observed in RMSD values was found to be under ~0.78 and ~0.56 nm for A1 and A3, respectively, which is considered to be very small and strongly suggest that the both complexes reached equilibration state during the simulation.

Another important parameter, Rg explains the rigidity and compactness of the entire protein-ligand complex and derived from the MD simulation trajectories. The Rg is the mass-weighted RMS (root-mean-square) distance of a collection of atoms from their common center of mass [71]. Overall dimensions and the change of protein structure during the MD simulation can be enlighted by the Rg parameter. The change in the structure of a protein during MD simulations can be quantified by the radius of gyration. The consistent variation in the Rg can explain that all protein-ligand complex was steadily folded throughout the simulation events, while little bit deviation observed for compound A1, during ~30–80 ns time period. Although such observation was noticed but considering the range of deviation (~2.07–2.17) it can be explained that for firmly folding the protein structure with the association of compound A1, such deviation was negotiable. Average, maximum and minimum Rg values obtained in MD simulation studies for all protein-ligand systems are given in Table 2. It can be observed that Rg values of all systems oscillated from 1.952 to 2.065 nm. The differences between the maximum and minimum Rg of CDK2 was found to be 0.203, 0.071, 0.117, 0.065 and 0.098 nm complex with A1, A2, A3, A4 and Dinaciclib, respectively. The Rg value of each frame was recorded and plotted

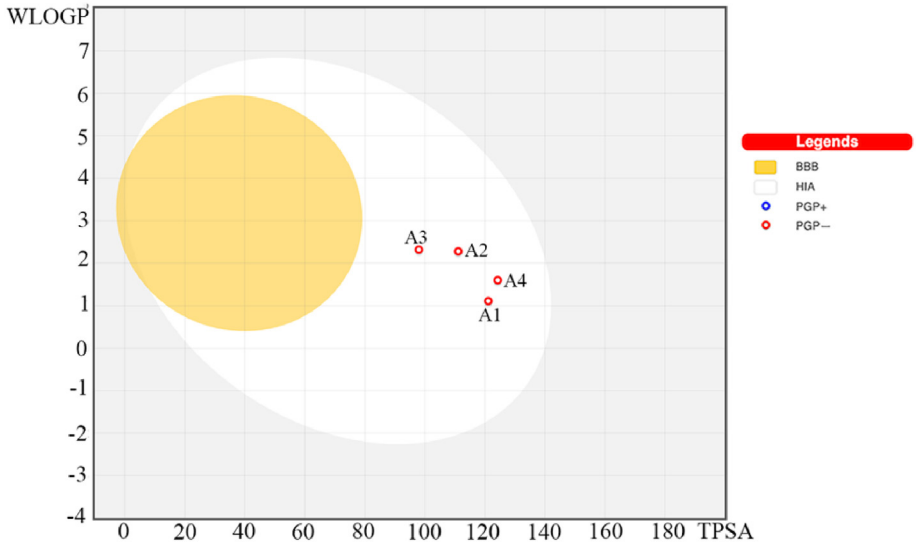

Fig. 5. The EGG-BOILED model for the final screened CDK2 inhibitors.

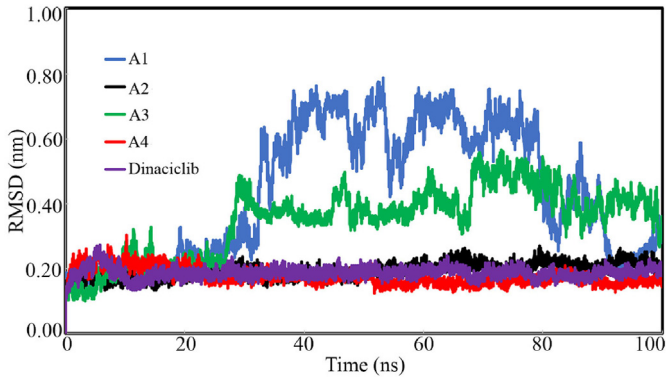

Fig. 6. The RMSD of the CDK2 backbone atoms over time bound with A1, A2, A3, A4 and Dinaciclib.

Table 2
Average, maximum and minimum RMSD, RMSF and Rg of A1, A2, A3, A4 and Dinaciclib complex with CDK2.

Molecule		RMSD (nm)	RMSF (nm)	Rg (nm)
A1	Average	0.436	0.209	2.065
	Maximum	0.787	2.433	2.170
	Minimum	0.000	0.067	1.967
A2	Average	0.195	0.126	2.023
	Maximum	0.270	0.584	2.058
	Minimum	0.000	0.041	1.987
A3	Average	0.348	0.171	2.035
	Maximum	0.566	1.613	2.102
	Minimum	0.001	0.050	1.985
A4	Average	0.175	0.134	2.004
	Maximum	0.304	0.672	2.037
	Minimum	0.000	0.040	1.972
Dinaciclib	Average	0.187	0.124	2.012
	Maximum	0.273	0.522	2.050
	Minimum	0.000	0.042	1.952

against the time of MD simulation (Fig. 7). The above observations clearly explained that CDK2 was remained consistent and rigid during the MD simulation. From Fig. 7, it can be seen that all compounds were reflected alike Rg profile, only observable fact counted as CDK2 bound with compound A1 deviated a little bit higher in comparison to others, however not exceeded beyond 2.17 nm. Therefore, it can be stated that the binding of the proposed molecules was unable to disturb the CDK2 protein system.

The RMSF parameter measures the average deviation of each protein residue over time from the reference position. In particular, RMSF analyzes the specific part of the protein structure that are fluctuating from its mean structure. During MD simulation, higher RMSF values of the protein indicate greater flexibility attained by the complex, whereas lower RMSF indicates lesser flexibility for the complex. The consistency of any protein molecule bound with a small molecule can be assessed by the exploration of RMSF of each amino acid. RMSF of each amino residue of CDK2 bound with A1, A2, A3, A4 and Dinaciclib was recorded and displayed in Fig. 8. Average, maximum and minimum RMSF values were calculated and given in Table 2. The differences between maximum and average can give an idea about the overall fluctuation of the system. The value of the differences between maximum and average was found to be 2.224, 0.458, 1.442, 0.538 and 0.398 nm for the complex with A1, A2, A3, A4 and Dinaciclib, respectively. Observed low values for RMSF undoubtedly explained that amino acid residues did not fluctuate much when bound with proposed molecules.

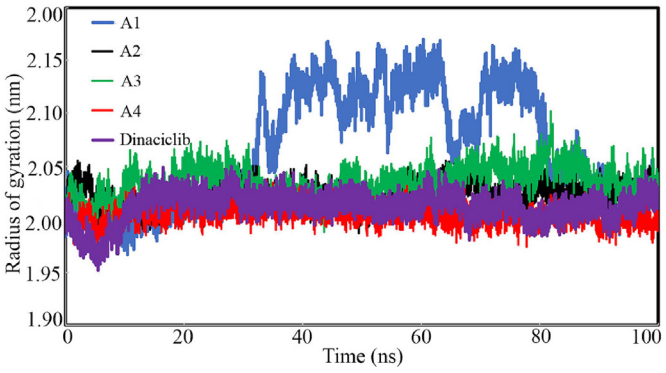

Fig. 7. Rg of CKD2 with A1, A2, A3, A4 and Dinaciclib complex.

3.6. Binding free energy analyses using MM-PBSA

The entire set of trajectories derived in 100 ns MD simulation was considered to calculate the binding free energy (ΔG_{bind}) of proposed molecules and Dinaciclib towards the CDK2. Among several methods, the MM-PBSA is one of the crucial and almost accurate approaches to obtain ΔG_{bind} from the MD simulation trajectories. It is also reported that ΔG_{bind} calculated through MM-PBSA approach more efficient and acceptable in comparison to molecular docking based binding energy. Two important energy components such as van der Waals and electrostatic were involved in the total ΔG_{bind} contribution.

Average, maximum and minimum of van der Waals, electrostatic and total binding free energies were recorded and given in Table 3. Total ΔG_{bind} of each frame was plotted against the time of MD simulation and given in Fig. 9. On detail analysis it can be seen that the highest average binding free energy was shown by A1 followed by Dinaciclib, A3, A4 and A2 with −991.831, −270.396, −257.075, −239.203, −210.452 kJ/mol, respectively. The above data was clearly explained that all molecules were shown a strong binding affinity towards the CDK2. It can also be seen that both energy components, van der Waals and electrostatic of all molecules except A1 were contributed more or less equally towards the total binding energy. Almost equal contributions of both van der Waals and electrostatic in A2, A3 and A4 were undoubtedly indicated that the presence of polar and non-polar substituents in these molecules critical for binding to the receptor cavity of the CDK2. In the case of A1, charged functional groups might be more important than non-polar for strong binding interactions. Therefore, binding energy analyses were clearly pointed out that all molecules consist of important functional components to form a stable complex with CDK2.

4. Future prospects

Chemical compounds derived from the food components are a rich source of pharmaceutical therapeutics. Exploration of drug-like chemical entities is extremely resource and time consuming along with the expensive process. Pharmacoinformatics approaches including virtual screening, molecular docking and molecular dynamics are already proven pioneer in drug discovery and research. The application of pharmacoinformatics methods in food components is an excellent strategy to find out lead-likeness chemical entities for a specific target. Although pharmacoinformatics stratagems become crucial and critical phenomenathere is an extreme and absolute need for experimental validation. Proposed CDK2 molecules through computation drug discovery need to assess a number of experimental approaches. The thermal shift assay can be used to detect the binding interactions between the catalytic amino residues of CDK2 and proposed small molecules. The binding affinity of the final molecules can be explored through the thermal melt assay approach. Detailed binding and unbinding events also can be verified through the kinetic study. Based on outcomes from the above experiments the molecules can be optimized and improved further to enhance the therapeutic effects.

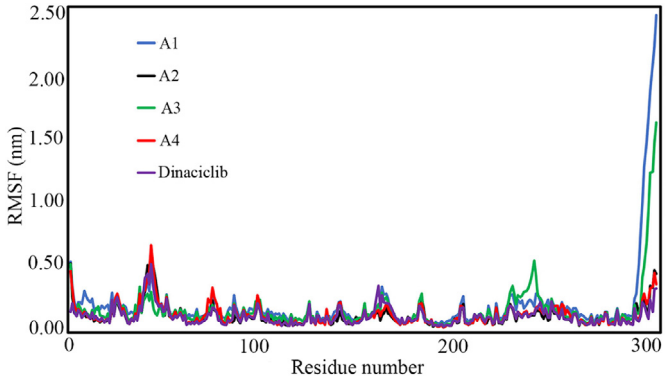

Fig. 8. RMSF vs. time of simulation of CDK2 complex with A1, A2, A3, A4 and Dinaciclib.

Table 3
Average binding free energies, van der Waals, and electrostatic energies of A1, A2, A3, A4 and Dinaciclib obtained in MM-PBSA method.

Molecule	Protein-ligand energies (kJ/mol)			
		van der Waals	Electrostatic	Total (ΔG_{bind})
A1	Average	−74.166	−917.665	−991.831
	Maximum	0.614	−241.495	−279.138
	Minimum	−129.279	−1536.763	−1630.911
A2	Average	−107.737	−102.715	−210.452
	Maximum	−54.734	−5.016	−81.536
	Minimum	−165.997	−251.689	−345.071
A3	Average	−109.938	−147.137	−257.075
	Maximum	−45.494	−10.539	−115.535
	Minimum	−154.499	−347.755	−434.343
A4	Average	−116.126	−123.077	−239.203
	Maximum	−52.454	−9.722	−94.836
	Minimum	−178.127	−229.315	−348.815
Dinaciclib	Average	−168.707	−101.689	−270.396
	Maximum	−102.162	31.390	−121.486
	Minimum	−246.106	−322.143	−545.649

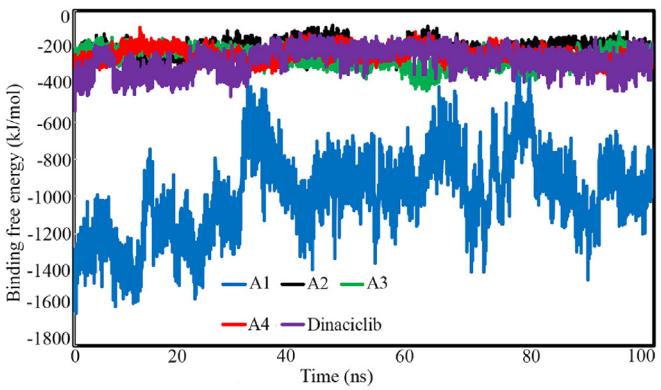

Fig. 9. Binding free energy vs time of A1, A2, A3, A4 and Dinaciclib.

5. Conclusion

A curated dataset of food components was screened through the multi-step molecular docking via VSW utility implemented Maestro suite. The standard CDK2 molecule, Dinaciclib was considered as a control parameter. Binding energy and molecular interactions profile were initially used to reduce the chemical space. Further, the *in-silico* pharmacokinetic characteristics were used to wipe out the inactive molecules targeting the CDK2. Finally, four potential chemical molecules were found crucial for successful inhibition of CDK2 for therapeutic application in cancer. Pharmacokinetics and drug-likeness properties were explored and found that final molecules possess lead-like behavior. The binding interaction in molecular docking study was revealed that all proposed molecules efficient enough to form a number of strong binding interactions. The stability of the complex between CDK2 and proposed molecules was assessed through MD simulation study. A

number of parameters were derived from the MD simulation trajectories and found that CDK2 remained consistent during the conformational analysis. The binding free energy of all molecules was derived through a widely used and acceptable MM-GBSA approach. High binding free energy was found for all the molecules which undoubtedly substantiated that proposed molecules possess a strong affinity towards the CDK2. Therefore, the above discussion clearly indicated that proposed molecules derived from the FooDB can be potential inhibitors for CDK2 subjected to experimental evaluation.

Computational resource

The CHPC (www.chpc.ac.za), Cape Town, South Africa is thankfully acknowledged for computational resources and tools.

Declaration of competing interest

Authors declare that there is no competing interest.

CRediT authorship contribution statement

Shovonlal Bhowmick: Data curation, Formal analysis, Investigation, Methodology, Writing - original draft, Writing - review & editing. **Nora Abdullah AlFaris:** Conceptualization, Writing - review & editing. **Jozaa Zaidan ALTamimi:** Conceptualization, Writing - review & editing. **Zeid A. ALOthman:** Conceptualization, Writing - review & editing. **Tahany Saleh Aldayel:** Conceptualization, Writing - review & editing. **Saikh Mohammad Wabaidur:** Conceptualization, Writing - review & editing. **Md Ataul Islam:** Conceptualization, Investigation, Supervision, Data curation, Writing - original draft, Writing - review & editing.

Acknowledgment

This work was funded by the Deanship of Scientific Research at Princess Nourah bint Abdulrahman University, Riyadh, Saudi Arabia through the Research Groups Program Grant no. (RGP-1440-0021).

Appendix A. Supplementary data

Supplementary data related to this article can be found at https://doi.org/10.1016/j.molstruc.2020.128316.

References

[1] H. Cory, S. Passarelli, J. Szeto, M. Tamez, J. Mattei, The role of polyphenols in human health and food systems: a mini-review, Frontiers in Nutrition 5 (87) (2018).
[2] D. Mozaffarian, Dietary and policy priorities for cardiovascular disease, diabetes, and obesity: a comprehensive review, Circulation 133 (2) (2016) 187–225.
[3] C. Nediani, J. Ruzzolini, A. Romani, L. Calorini, Oleuropein, a bioactive compound from olea europaea L., as a potential preventive and therapeutic agent in non-communicable diseases, Antioxidants 8 (12) (2019) 578.
[4] B.M. Burton-Freeman, A.K. Sandhu, I. Edirisinghe, Red raspberries and their bioactive polyphenols: cardiometabolic and neuronal health links, Advances in Nutrition 7 (1) (2016) 44–65.
[5] A. Parihar, M.S. Parihar, Bioactive food components in the prevention of cardiovascular diseases, in: J.-M. Mérillon, K.G. Ramawat (Eds.), Bioactive Molecules in Food, Springer International Publishing, Cham, 2017, pp. 1–21.
[6] T.C. Wallace, R.L. Bailey, J.B. Blumberg, B. Burton-Freeman, C.O. Chen, K.M. Crowe-White, A. Drewnowski, S. Hooshmand, E. Johnson, R. Lewis, R. Murray, S.A. Shapses, D.D. Wang, Fruits, vegetables, and health: a comprehensive narrative, umbrella review of the science and recommendations for enhanced public policy to improve intake, Crit. Rev. Food Sci. Nutr. (2019) 1–38.
[7] T.D. Natarajan, J.R. Ramasamy, K. Palanisamy, Nutraceutical potentials of synergic foods: a systematic review, Journal of Ethnic Foods 6 (1) (2019) 27.
[8] M. Konstantinidi, A.E. Koutelidakis, Functional foods and bioactive compounds: a review of its possible role on weight management and obesity's metabolic consequences, Medicines (Basel) 6 (3) (2019).
[9] M.M.G. Karasawa, C. Mohan, Fruits as prospective reserves of bioactive compounds: a review, Natural products and bioprospecting 8 (5) (2018) 335–346.
[10] D. Cianciosi, A. Varela-Lopez, T.Y. Forbes-Hernandez, M. Gasparrini, S. Afrin, P. Reboredo-Rodriguez, J. Zhang, J.L. Quiles, S.F. Nabavi, M. Battino, F. Giampieri, Targeting molecular pathways in cancer stem cells by natural bioactive compounds, Pharmacol. Res. 135 (2018) 150–165.
[11] M.J. Rein, M. Renouf, C. Cruz-Hernandez, L. Actis-Goretta, S.K. Thakkar, M. da Silva Pinto, Bioavailability of bioactive food compounds: a challenging journey to bioefficacy, Br. J. Clin. Pharmacol. 75 (3) (2013) 588–602.
[12] M.M. Ulaszewska, C.H. Weinert, A. Trimigno, R. Portmann, C. Andres Lacueva, R. Badertscher, L. Brennan, C. Brunius, A. Bub, F. Capozzi, M. Cialiè Rosso, C.E. Cordero, H. Daniel, S. Durand, B. Egert, P.G. Ferrario, E.J.M. Feskens, P. Franceschi, M. Garcia-Aloy, F. Giacomoni, P. Giesbertz, R. González-Domínguez, K. Hanhineva, L.Y. Hemeryck, J. Kopka, S.E. Kulling, R. Llorach, C. Manach, F. Mattivi, C. Migné, L.H. Münger, B. Ott, G. Picone, G. Pimentel, E. Pujos-Guillot, S. Riccadonna, M.J. Rist, C. Rombouts, J. Rubert, T. Skurk, P.S.C. Sri Harsha, L. Van Meulebroek, L. Vanhaecke, R. Vázquez-Fresno, D. Wishart, G. Vergères, Nutrimetabolomics: an integrative action for metabolomic analyses in human nutritional studies, Mol. Nutr. Food Res. 63 (1) (2019) 1800384.
[13] C. Tiffon, The impact of nutrition and environmental epigenetics on human health and disease, Int. J. Mol. Sci. 19 (11) (2018).
[14] L. Silva, N. Pinheiro-Castro, G.M. Novaes, G.F.L. Pascoal, T.P. Ong, Bioactive food compounds, epigenetics and chronic disease prevention: focus on early-life interventions with polyphenols, Food Res. Int. 125 (2019) 108646.
[15] S.W. Choi, S. Friso, Epigenetics: a new bridge between nutrition and health, Adv Nutr 1 (1) (2010) 8–16.
[16] T.M. Hardy, T.O. Tollefsbol, Epigenetic diet: impact on the epigenome and cancer, Epigenomics 3 (4) (2011) 503–518.
[17] A.R. Vandiver, A. Idrizi, L. Rizzardi, A.P. Feinberg, K.D. Hansen, DNA methylation is stable during replication and cell cycle arrest, Sci. Rep. 5 (1) (2015) 17911.
[18] C. Desjobert, M. El Mai, T. Gerard-Hirne, D. Guianvarc'h, A. Carrier, C. Pottier, P.B. Arimondo, J. Riond, Combined analysis of DNA methylation and cell cycle in cancer cells, Epigenetics 10 (1) (2015) 82–91.
[19] J.A. Milner, Molecular targets for bioactive food components, J. Nutr. 134 (9) (2004) 2492S–2498S.
[20] R. Visconti, R. Della Monica, D. Grieco, Cell cycle checkpoint in cancer: a therapeutically targetable double-edged sword, J. Exp. Clin. Canc. Res. 35 (1) (2016) 153.
[21] K. Collins, T. Jacks, N.P. Pavletich, The cell cycle and cancer, Proc. Natl. Acad. Sci. Unit. States Am. 94 (7) (1997) 2776–2778.
[22] G.H. Williams, K. Stoeber, The cell cycle and cancer, J. Pathol. 226 (2) (2012) 352–364.
[23] K.J. Barnum, M.J. O'Connell, Cell cycle regulation by checkpoints, Methods Mol. Biol. 1170 (2014) 29–40.
[24] S. Tadesse, E.C. Caldon, W. Tilley, S. Wang, Cyclin-dependent kinase 2 inhibitors in cancer therapy: an update, J. Med. Chem. 62 (9) (2019) 4233–4251.
[25] E.J. Chenette, A key role for CDK2, Nat. Rev. Canc. 10 (2) (2010), 84-84.
[26] X. He, H. Xiang, X. Zong, X. Yan, Y. Yu, G. Liu, D. Zou, H. Yang, CDK2-AP1 inhibits growth of breast cancer cells by regulating cell cycle and increasing docetaxel sensitivity in vivo and in vitro, Canc. Cell Int. 14 (1) (2014) 130.
[27] S. Tadesse, A.T. Anshabo, N. Portman, E. Lim, W. Tilley, C.E. Caldon, S. Wang, Targeting CDK2 in cancer: challenges and opportunities for therapy, Drug Discov. Today 25 (2) (2019) 406–413.
[28] M. Kawakami, L.M. Mustachio, J. Rodriguez-Canales, B. Mino, J. Roszik, P. Tong, J. Wang, J.J. Lee, J.H. Myung, J.V. Heymach, F.M. Johnson, S. Hong, L. Zheng, S. Hu, P.A. Villalobos, C. Behrens, I. Wistuba, S. Freemantle, X. Liu, E. Dmitrovsky, Next-generation CDK2/9 inhibitors and anaphase catastrophe in lung cancer, JNCI: J. Natl. Cancer Inst. 109 (6) (2017).
[29] X.N. Shi, H. Li, H. Yao, X. Liu, L. Li, K.S. Leung, H.F. Kung, M.C. Lin, Adapalene inhibits the activity of cyclin-dependent kinase 2 in colorectal carcinoma, Mol. Med. Rep. 12 (5) (2015) 6501–6508.
[30] J. Wang, T. Yang, G. Xu, H. Liu, C. Ren, W. Xie, M. Wang, Cyclin-dependent kinase 2 promotes tumor proliferation and induces radio resistance in glioblastoma, Translational oncology 9 (6) (2016) 548–556.
[31] A.C. Faber, T.C. Chiles, Inhibition of cyclin-dependent kinase-2 induces apoptosis in human diffuse large B-cell lymphomas, Cell Cycle 6 (23) (2007) 2982–2989.
[32] X. Yin, J. Yu, Y. Zhou, C. Wang, Z. Jiao, Z. Qian, H. Sun, B. Chen, Identification of CDK2 as a novel target in treatment of prostate cancer, Future Oncol. 14 (8) (2018) 709–718.
[33] S.R. Whittaker, C. Barlow, M.P. Martin, C. Mancusi, S. Wagner, A. Self, E. Barrie, R. Te Poele, S. Sharp, N. Brown, S. Wilson, W. Jackson, P.M. Fischer, P.A. Clarke, M.I. Walton, E. McDonald, J. Blagg, M. Noble, M.D. Garrett, P. Workman, Molecular profiling and combinatorial activity of CCT068127: a potent CDK2 and CDK9 inhibitor, Molecular Oncology 12 (3) (2018) 287–304.
[34] S. Ali, D.A. Heathcote, S.H. Kroll, A.S. Jogalekar, B. Scheiper, H. Patel, J. Brackow, A. Siwicka, M.J. Fuchter, M. Periyasamy, R.S. Tolhurst, S.K. Kanneganti, J.P. Snyder, D.C. Liotta, E.O. Aboagye, A.G. Barrett, R.C. Coombes, The development of a selective cyclin-dependent kinase inhibitor that shows antitumor activity, Canc. Res. 69 (15) (2009) 6208–6215.
[35] M.E. Noble, J.A. Endicott, L.N. Johnson, Protein kinase inhibitors: insights into

drug design from structure, Science 303 (5665) (2004) 1800–1805.
[36] R. Martín-Hernández, G. Reglero, J.M. Ordovás, A. Dávalos, NutriGenomeDB: a Nutrigenomics Exploratory and Analytical Platform, Database (2019) 2019.
[37] R. Martín-Hernández, G. Reglero, A. Dávalos, Data mining of nutrigenomics experiments: identification of a cancer protective gene signature, Journal of Functional Foods 42 (2018) 380–386.
[38] M. Peyressatre, C. Prevel, M. Pellerano, M.C. Morris, Targeting cyclin-dependent kinases in human cancers: from small molecules to Peptide inhibitors, Cancers 7 (1) (2015) 179–237.
[39] A. Echalier, A.J. Hole, G. Lolli, J.A. Endicott, M.E. Noble, An inhibitor's-eye view of the ATP-binding site of CDKs in different regulatory states, ACS Chem. Biol. 9 (6) (2014) 1251–1256.
[40] M. Malumbres, Cyclin-dependent kinases, Genome Biol. 15 (6) (2014) 122.
[41] Virtual Screening Workflow: Maestro, Schrödinger, LLC, New York, 2019.
[42] N.M. O'Boyle, M. Banck, C.A. James, C. Morley, T. Vandermeersch, G.R. Hutchison, Open Babel: an open chemical toolbox, J. Cheminf. 3 (2011) 33.
[43] E.P. Jane, D.R. Premkumar, J.M. Cavaleri, P.A. Sutera, T. Rajasekar, I.F. Pollack, Dinaciclib, a cyclin-dependent kinase inhibitor promotes proteasomal degradation of mcl-1 and enhances ABT-737-mediated cell death in malignant human glioma cell lines, J. Pharmacol. Exp. Therapeut. 356 (2) (2016) 354–365.
[44] G.M. Sastry, M. Adzhigirey, T. Day, R. Annabhimoju, W. Sherman, Protein and ligand preparation: parameters, protocols, and influence on virtual screening enrichments, J. Comput. Aided Mol. Des. 27 (3) (2013) 221–234.
[45] M.P. Martin, S.H. Olesen, G.I. Georg, E. Schonbrunn, Cyclin-dependent kinase inhibitor dinaciclib interacts with the acetyl-lysine recognition site of bromodomains, ACS Chem. Biol. 8 (11) (2013) 2360–2365.
[46] G. Kontopidis, C. McInnes, S.R. Pandalaneni, I. McNae, D. Gibson, M. Mezna, M. Thomas, G. Wood, S. Wang, M.D. Walkinshaw, P.M. Fischer, Differential binding of inhibitors to active and inactive CDK2 provides insights for drug design, Chem. Biol. 13 (2) (2006) 201–211.
[47] T.G. Davies, P. Tunnah, L. Meijer, D. Marko, G. Eisenbrand, J.A. Endicott, M.E.M. Noble, Inhibitor binding to active and inactive CDK2: the crystal structure of CDK2-cyclin A/Indirubin-5-Sulphonate, Structure 9 (5) (2001) 389–397.
[48] J. Chen, L. Pang, W. Wang, L. Wang, J.Z.H. Zhang, T. Zhu, Decoding molecular mechanism of inhibitor bindings to CDK2 using molecular dynamics simulations and binding free energy calculations, J. Biomol. Struct. Dyn. 38 (4) (2020) 985–996.
[49] E. Schonbrunn, S. Betzi, R. Alam, M.P. Martin, A. Becker, H. Han, R. Francis, R. Chakrasali, S. Jakkaraj, A. Kazi, S.M. Sebti, C.L. Cubitt, A.W. Gebhard, L.A. Hazlehurst, J.S. Tash, G.I. Georg, Development of highly potent and selective diaminothiazole inhibitors of cyclin-dependent kinases, J. Med. Chem. 56 (10) (2013) 3768–3782.
[50] Schrödinger Release 2019-2, Maestro, Schrödinger, LLC, New York, NY, 2019.
[51] T.A. Halgren, R.B. Murphy, R.A. Friesner, H.S. Beard, L.L. Frye, W.T. Pollard, J.L. Banks, Glide: a new approach for rapid, accurate docking and scoring. 2. Enrichment factors in database screening, J. Med. Chem. 47 (7) (2004) 1750–1759.
[52] R.A. Friesner, R.B. Murphy, M.P. Repasky, L.L. Frye, J.R. Greenwood, T.A. Halgren, P.C. Sanschagrin, D.T. Mainz, Extra precision glide: docking and scoring incorporating a model of hydrophobic enclosure for protein-ligand complexes, J. Med. Chem. 49 (21) (2006) 6177–6196.
[53] A. Daina, O. Michielin, V. Zoete, SwissADME: a free web tool to evaluate pharmacokinetics, drug-likeness and medicinal chemistry friendliness of small molecules, Sci. Rep. 7 (2017) 42717.
[54] C.A. Lipinski, F. Lombardo, B.W. Dominy, P.J. Feeney, Experimental and computational approaches to estimate solubility and permeability in drug discovery and development settings, Adv. Drug Deliv. Rev. 46 (1–3) (2001) 3–26.
[55] R. Kumari, R. Kumar, A. Lynn, g_mmpbsa—a GROMACS tool for high-throughput MM-PBSA calculations, J. Chem. Inf. Model. 54 (7) (2014) 1951–1962.
[56] M.A. Islam, T.S. Pillay, beta-secretase inhibitors for Alzheimer's disease: identification using pharmacoinformatics, J. Biomol. Struct. Dyn. 37 (2) (2019) 503–522.
[57] M.O. Taha, M. Habash, Z. Al-Hadidi, A. Al-Bakri, K. Younis, S. Sisan, Docking-based comparative intermolecular contacts analysis as new 3-D QSAR concept for validating docking studies and in silico screening: NMT and GP inhibitors as case studies, J. Chem. Inf. Model. 51 (3) (2011) 647–669.
[58] H.C. Tang, C.Y. Chen, Drug design of cyclin-dependent kinase 2 inhibitor for melanoma from traditional Chinese medicine, BioMed Res. Int. 2014 (2014) 798742.
[59] R. Roskoski Jr., Cyclin-dependent protein serine/threonine kinase inhibitors as anticancer drugs, Pharmacol. Res. 139 (2019) 471–488.
[60] M.P. Martin, S.H. Olesen, G.I. Georg, E. Schönbrunn, Cyclin-dependent kinase inhibitor dinaciclib interacts with the acetyl-lysine recognition site of bromodomains, ACS Chem. Biol. 8 (11) (2013) 2360–2365.
[61] P. Mahajan, G. Chashoo, M. Gupta, A. Kumar, P.P. Singh, A. Nargotra, Fusion of structure and ligand based methods for identification of novel CDK2 inhibitors, J. Chem. Inf. Model. 57 (8) (2017) 1957–1969.
[62] S.K. Tripathi, S.K. Singh, P. Singh, P. Chellaperumal, K.K. Reddy, C. Selvaraj, Exploring the selectivity of a ligand complex with CDK2/CDK1: a molecular dynamics simulation approach, J. Mol. Recogn. : JMR (J. Mol. Recognit.) 25 (10) (2012) 504–512.
[63] P.M. Clare, R.A. Poorman, L.C. Kelley, K.D. Watenpaugh, C.A. Bannow, K.L. Leach, The cyclin-dependent kinases cdk2 and cdk5 act by a random, anticooperative kinetic mechanism, J. Biol. Chem. 276 (51) (2001) 48292–48299.
[64] Y. Li, J. Zhang, W. Gao, L. Zhang, Y. Pan, S. Zhang, Y. Wang, Insights on structural characteristics and ligand binding mechanisms of CDK2, Int. J. Mol. Sci. 16 (5) (2015) 9314–9340.
[65] M. Otyepka, I. Bartova, Z. Kriz, J. Koca, Different mechanisms of CDK5 and CDK2 activation as revealed by CDK5/p25 and CDK2/cyclin A dynamics, J. Biol. Chem. 281 (11) (2006) 7271–7281.
[66] S. Vukovic, P.E. Brennan, D.J. Huggins, Exploring the role of water in molecular recognition: predicting protein ligandability using a combinatorial search of surface hydration sites, J. Phys. Condens. Matter 28 (34) (2016) 344007.
[67] L. Duan, G. Feng, X. Wang, L. Wang, Q. Zhang, Effect of electrostatic polarization and bridging water on CDK2-ligand binding affinities calculated using a highly efficient interaction entropy method, Phys. Chem. Chem. Phys. 19 (15) (2017) 10140–10152.
[68] R. Jia, L.J. Yang, S.Y. Yang, Binding energy contributions of the conserved bridging water molecules in CDK2-inhibitor complexes: a combined QM/MM study, Chem. Phys. Lett. 460 (1) (2008) 300–305.
[69] G. Klopmand, Concepts and applications of molecular similarity, in: Mark A. Johnson, Gerald M. Maggiora (Eds.), John Wiley & Sons, New York, 1990, p. 393. Price: $65.00, Journal of Computational Chemistry 13(4) (1992) 539-540.
[70] T.W. Backman, Y. Cao, T. Girke, ChemMine tools: an online service for analyzing and clustering small molecules, Nucleic Acids Res. 39 (2011) W486–W491. Web Server issue).
[71] M.H. Baig, D.R. Sudhakar, P. Kalaiarasan, N. Subbarao, G. Wadhawa, M. Lohani, M.K. Khan, A.U. Khan, Insight into the effect of inhibitor resistant S130G mutant on physico-chemical properties of SHV type beta-lactamase: a molecular dynamics study, PloS One 9 (12) (2014), e112456.